

Effects of nonsinusoidal character of atomic modulation on NQR spin-lattice relaxation time of incommensurate phases

Silvina C. Pérez, Clemar Schurrer, and Alberto Wolfenson

Facultad de Matemática, Astronomía y Física, Universidad Nacional de Córdoba, Ciudad Universitaria, 5000 Córdoba, Argentina

(Received 21 December 2000; revised manuscript received 9 March 2001; published 21 May 2001)

The present work is an extension of the theoretical calculation developed by Blinc to explain the temperature and frequency dependence of the spin-lattice relaxation time in incommensurate phases. We have evaluated the influence of the nonsinusoidal character of the atomic modulation, in the linear approximation, over the NQR spectra and over the spin-lattice relaxation due to direct and Raman processes. It is shown that the peak with lower intensity in the NQR spectra always has a larger T_1 and viceversa. The results have been applied to bis(4-chlorophenyl)sulfone T_1 and line-shape data. The temperature and frequency dependence of T_1 are well reproduced if Raman processes are considered.

DOI: 10.1103/PhysRevB.63.224411

PACS number(s): 76.60.Gv, 64.70.Rh

I. INTRODUCTION

Some crystals undergo a structural phase transition from high-temperature normal (N) phase to a structurally incommensurate (IC) modulated phase at a certain transition temperature T_I . The theory that describes the IC phase predicts that the soft mode of the N phase splits in the IC phase into an acousticlike phason branch and an opticlike amplitudon branch. These modes give the main contribution to the nuclear quadrupolar resonance (NQR) spin-lattice relaxation time T_1 and both contribute differently at different parts of the inhomogeneous NQR line spectra. In fact Blinc¹ has evaluated the temperature and frequency dependence of the nuclear spin-lattice relaxation rate in “the plane-wave modulation limit” where the incommensurate distortion is characterized by a single Fourier component of the displacement

$$\langle u(x) \rangle = \sqrt{2}A \cos(q_s x + \phi_o) \quad (1)$$

and a linear relation between the observed NQR frequency and $u(x)$ is proposed. This model shows that at both edges of the inhomogeneous NQR spectra the amplitudon branch gives the same and unique contribution to T_1 , while the phason contribution is observed at the center of the spectra. Also, in this model, the inhomogeneous NQR spectra is symmetric with respect to the center of the line.

Even when the plane-wave limit can describe some systems, it is well known that others harmonics can appear in the IC modulation.² One of these systems is the IC phase of the bis(4-chlorophenyl)sulfone (BCPS). This compound has an IC phase below $T_I=150$ K widely studied by different experimental techniques like NQR,^{3,4} x-ray,⁵ neutron scattering,⁶ etc. In fact, a careful structural analysis of the IC phase of BCPS performed by means of x-ray diffraction,⁵ has demonstrated the nonsinusoidal character of the atomic modulation, therefore at least the second-order harmonic has to be considered in a model of the IC distortion. This is

$$\langle u(x) \rangle = \sqrt{2}[A \cos(q_s x + \phi_o) + B \cos(2q_s x + \psi_o)]. \quad (2)$$

The goal of the present work is to calculate the effect that this nonsinusoidal atomic modulation has on the frequency

and temperature dependence of T_1 . The model is applied to the analysis of BCPS T_1 data as well as to the spectral-line density $f(\nu)$.

II. EXPERIMENT

The specimen of bis(4-chlorophenyl)sulfone was the pure one from Fluka. The material was purified by zone melting for about twice. The sample container was a cylinder of 1 cm diameter, the amount of sample used was about 2 g. ³⁵Cl NQR measurements were done using a Fourier-transform pulse spectrometer with a Tecmag NMRkit II multinuclei observe unit and a Tecmag Macintosh-based real-time NMR station. The line shape was obtained from the fast-Fourier-transform echo $\pi/2$ - π reconstruction method.³ T_1 measurements were made upon the echo by the standard two-pulse $\pi/2$ - $\pi/2$ sequence. The temperature range covered was from 80 K up to the melting point. A LakeShore temperature controller was used for providing temperature stability of the sample better than 0.1 K.

III. THEORY

In order to evaluate the spin-lattice relaxation rates it is necessary to express the nuclear displacements in terms of normal modes of the incommensurate lattice. Bruce and Cowley⁷ described these normal modes when the displacement field can be expressed in terms of its Fourier components. Following their calculations and using their notation, it results that the associated eigendistortions in terms of the amplitudes $[Q(\mathbf{q})]$ of the Fourier component of the displacement field $u(x)$ are

$$P_1 = \frac{\alpha}{\sqrt{2}}(e^{i\phi}Q_1 + e^{-i\phi}Q_2 - \gamma_1 e^{3i\phi}Q_3 - \gamma_1 e^{-i\phi}Q_4), \quad (3)$$

$$P_2 = \frac{\alpha i}{\sqrt{2}}(-e^{i\phi}Q_1 + e^{-i\phi}Q_2 + \gamma_1 e^{i\phi}Q_3 - \gamma_1 e^{-3i\phi}Q_4),$$

$$P_3 = \frac{\alpha}{\sqrt{2}} (\gamma_1 Q_1 + \gamma_1 e^{-2i\phi} Q_2 + e^{2i\phi} Q_3 + e^{-2i\phi} Q_4),$$

$$P_4 = \frac{\alpha i}{\sqrt{2}} (-\gamma_1 e^{2i\phi} Q_1 + \gamma_1 Q_2 - e^{2i\phi} Q_3 + e^{-2i\phi} Q_4)$$

with

$$\alpha = \frac{1}{\sqrt{1 + \gamma_1^2}} \approx 1, \quad \gamma_1 = \frac{3\sqrt{2}v_o}{\omega^2(2q_s)} \sqrt{\frac{|r_o|}{4u_o}} = -\frac{2B}{A},$$

$$r_o \propto T - T_l. \quad (4)$$

The spatial-fluctuation profile associated with the coordinates Q_1 , Q_2 , Q_3 , and Q_4 can then be written as

$$\begin{aligned} \delta u(x) = & \sqrt{2} \{ (\delta P_1 + \gamma_1 \cos \phi_o \delta P_3) \cos(q_s x + \phi_o) \\ & + (\delta P_2 + \gamma_1 \cos \phi_o \delta P_4) \sin(q_s x + \phi_o) \\ & + (\delta P_3 - \gamma_1 \cos \phi_o \delta P_1) \cos(2q_s x + 2\phi_o) \\ & + (\delta P_4 - \gamma_1 \cos \phi_o \delta P_2) \sin(2q_s x + 2\phi_o) \}. \end{aligned} \quad (5)$$

It is instructive to compare this expression with the form of the fluctuation profile arising from spatial modulation of the amplitudes A and B and the phase angles ϕ_o and ψ_o ($\psi_o = 2\phi_o$). Assuming that the phase fluctuations are small, it gives

$$\begin{aligned} \delta u(x) = & \sqrt{2} [-A \delta \phi(x) \sin(q_s x + \phi_o) + \delta A \cos(q_s x + \phi_o) \\ & - B \delta \psi \sin(2q_s x + \psi_o) + \delta B \cos(2q_s x + \psi_o)]. \end{aligned} \quad (6)$$

Comparison of Eqs. (5) and (6) shows that, provided the phase fluctuations are small, the coordinates δP_1 , δP_2 , δP_3 , and δP_4 may be identified with a combination of local fluctuations in the amplitude and the phase of the displacement field. Using these relations, the expressions for A and B reported by Bruce and Cowley,⁷ and including contributions up to $O(v_o^2)$, it is possible to obtain

$$\delta P_3 = \gamma_1 (1 + \cos \phi_o) \delta P_1, \quad \delta P_4 = \gamma_1 (1 + \cos \phi_o) \delta P_2. \quad (7)$$

The use of these relations provides, written in the time domain, the following spatial-fluctuation profile:

$$\begin{aligned} \delta u(t) = & 2\sqrt{2} \sum_k \{ [\cos(q_s x + \phi_o) + \gamma_1 \cos(2q_s x + 2\phi_o)] \\ & \times P_{1k}(t) + [\sin(q_s x + \phi_o) \\ & + \gamma_1 \sin(2q_s x + 2\phi_o)] P_{2k}(t) \} e^{-ikx}. \end{aligned} \quad (8)$$

As it was stated by Blinc,¹ the μ th component of the electric-field gradient (EFG) tensor at the l th lattice site $\Delta T^\mu(l, t)$ can be expressed as

$$\begin{aligned} \Delta T^\mu(l, t) = & \sum_i [T_{01}^\mu(l) + T_{02}^\mu(l) \mathbf{u}_j] \delta \mathbf{u}_i + \frac{1}{2} \sum_{i,j} T_{02}^\mu(l) \delta \mathbf{u}_i \\ & \otimes \delta \mathbf{u}_j + \dots, \end{aligned} \quad (9)$$

where $T_{01}^\mu(l)$ and $T_{02}^\mu(l)$ are the linear and quadratic terms of the Taylor expansion of the EFG tensor.

It is well known that the first term in Eq. (9) causes direct one-phonon spin-flip relaxation processes and it dominates relaxation if the normal modes are strongly overdamped, whereas the second term causes Raman two-phonon spin-flip processes and it dominates relaxation when the normal modes are damped or weakly damped.¹

A. Spin-lattice relaxation via direct process

In this case one can describe the relaxation process classically. Following Blinc and after some simple calculations, the spin-transition probability W^μ for the l th nucleus is given by

$$\begin{aligned} W_l^\mu = & \frac{2kT}{3\rho_l} \frac{e^4 Q^2}{h^2} |T_{01}^\mu(l) + T_{02}^\mu(l) \mathbf{u}_j|^2 \{ [X^2 + 2\gamma_1 X(2X^2 \\ & - 1)] J_A + [(1 - X^2) + 4\gamma_1(1 - X^2)X] J_\phi \} \end{aligned} \quad (10)$$

where

$$\omega_{\beta k}^2 = \omega_{\beta o}^2 + \kappa k^2, \quad J_\beta = \frac{\pi}{4} \kappa^{-3/2} \frac{\Gamma_\beta}{\omega_{\beta o}}, \quad \beta = A, \phi,$$

$$\omega_{A o}^2 = 2a(T_l - T), \quad X = \cos(q_s x + \phi_o) \quad (11)$$

for the limit in which the cutoff soft-mode frequency $\omega_{\beta \Lambda}$ —corresponding to the maximal \mathbf{k} value—is much larger than the soft-mode frequency $\omega_{\beta o}$ at $\mathbf{k} = \mathbf{0}$ and this is in turn large as compared to the NQR frequency. Γ_β and ρ_l are defined in Ref. 1.

B. Spin-lattice relaxation via Raman processes

In this case the transition probability is given by the well-known formula⁸

$$\begin{aligned} W_l^\mu = & \frac{2\pi}{\hbar^2} \int \int |\langle m, n_q + 1, n_{q'} | ED_l^\mu \Delta T_2^\mu(l) | m + \mu, n_q, n_{q'} + 1 \rangle|^2 \\ & \times \rho(\omega') \rho(\omega'') \delta(\omega' - \omega'' - \mu\omega) d\omega' d\omega''. \end{aligned} \quad (12)$$

One easily finds,

$$\begin{aligned} W_l^\mu = & \frac{2}{3\pi} \left| \frac{e^2 Q T_2^\mu}{\hbar} \right|^2 \left(\frac{KT}{\rho_l} \right)^2 \{ X^3 [X + 4\gamma_1(2X^2 - 1)] J_{AA} \\ & + (1 - X^2)^2 [1 + 8\gamma_1 X] J_{\phi\phi} \\ & + [X^2(1 - X^2) + 4\gamma_1 X^3(1 - X^2) \\ & + 2\gamma_1(1 - X^2)X(2X^2 - 1)] (J_{A\phi} + J_{\phi A}) \}, \end{aligned} \quad (13)$$

where

$$J_{\beta\beta'} = \kappa^{-3} \int_{\omega_{\beta o}}^{\omega_{\beta\Delta}} \sqrt{\left\{1 - \left(\frac{\omega_{\beta o}}{\omega + \omega'}\right)^2\right\} \left\{1 - \left(\frac{\omega_{\beta' o}}{\omega'}\right)^2\right\}} d\omega'. \quad (14)$$

Assuming the resonant frequency $\omega \ll \omega'$ gives

$$J_{\beta\beta'} \approx \kappa^{-3} (\omega_{\beta\Delta} - 2\omega_{\beta o}). \quad (15)$$

It is worth noting that expressions (10) and (13) for the transition probability agree with those obtained by Blinc when $\gamma_1 = 0$ (plane-wave limit).

C. Combined theoretical analysis of the spectral density and T_1 data

In the linear approximation, the NQR frequency for the axially symmetric case can be given by³

$$\nu = \nu_o + \nu_1 u = \nu_o + \nu_1 [AX + B(2X^2 - 1)]. \quad (16)$$

In this case, the spectral density $f(\nu) = (1/2\pi |d\nu/d\phi|)$, which is equal to the inhomogeneous line shape, will have singularities whenever $d\nu/d\phi$ becomes zero. In terms of X ,

$$f(X) = \frac{1}{2\pi A |\nu_1| \left|1 + 4\frac{B}{A}X\right| (1 - X^2)}. \quad (17)$$

Obviously the singularities occur for $X = \pm 1$ and $X = -A/4B$ if $A \leq 4B$. Since incommensurate line shapes usually present two well-defined singularities, we associate them with $X = \pm 1$ because the condition $A \leq 4B$ is more difficult to accomplish.

Evaluation of $f(X)$ close to $X = +1$ and close to $X = -1$, using the substitution $B/A = -\gamma_1/2$ gives

$$\lim_{X \rightarrow 1} f(X) = \frac{1}{2\pi A |\nu_1| |1 - 2\gamma_1| \varepsilon}, \quad (18)$$

$$\lim_{X \rightarrow -1} f(X) = \frac{1}{2\pi A |\nu_1| |1 + 2\gamma_1| \varepsilon},$$

with $\varepsilon \sim 0$.

After some simple algebra an expression for γ_1 is found

$$\gamma_1 = \frac{1}{2} \left[\frac{f(1) - f(-1)}{f(1) + f(-1)} \right], \quad (19)$$

which could be obtained from experimental data as a function of temperature

In the same way, for relaxation times, it is possible to write down

(a) direct processes

$$\frac{T_1(-1)}{T_1(1)} = \frac{|T_{01}^\mu(l) + (A+B)T_{02}^\mu(l)|^2 (1 + 2\gamma_1)}{|T_{01}^\mu(l) + (-A+B)T_{02}^\mu(l)|^2 (1 - 2\gamma_1)}. \quad (20)$$

(b) Raman processes

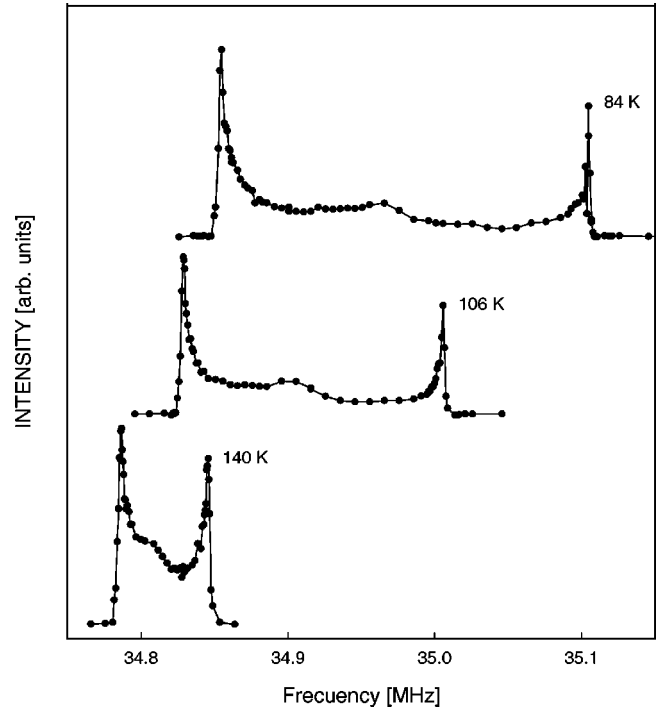


FIG. 1. ^{35}Cl NQR spectra of BCPS below T_I . These were obtained from the Fourier transform of the echo signal as a function of the irradiation frequency.

$$\frac{T_1(-1)}{T_1(1)} = \frac{1 + 4\gamma_1}{1 - 4\gamma_1}. \quad (21)$$

Depending on the sign of γ_1 , two situations are possible

$$\begin{aligned} \gamma_1 > 0 &\Rightarrow f(-1) < f(+1) \text{ and } T_1(-1) > T_1(+1), \\ \gamma_1 < 0 &\Rightarrow f(+1) < f(-1) \text{ and } T_1(-1) < T_1(+1). \end{aligned} \quad (22)$$

The concluding remark is that the peak of the spectra where the intensity is lower will always have a larger T_1 .

In the case where Raman processes dominate relaxation, γ_1 as a function of temperature can also be obtained from experimental T_1 data as

$$\gamma_1 = \frac{1}{4} \left[\frac{T_1(-1) - T_1(1)}{T_1(1) + T_1(-1)} \right]. \quad (23)$$

IV. EXPERIMENTAL RESULTS

Figure 1 shows some observed NQR spectra of BCPS at three different temperatures. It is observed that the intensity of the peaks is different, being higher at the lower frequency. On the other hand, Fig. 2 shows the temperature dependence of T_1 data from 80 K up to the melting point. This data are in good agreement with those previously reported by Schneider *et al.*⁴ T_1 data below $T \sim 150$ K were measured at both peaks of the NQR spectra. The highest T_1 value corresponds to the peak with high frequency and vice versa. In Fig. 3 γ_1 has been plotted as a function of temperature obtained from experimental data using Eq. (23). Figure 5 shows the fre-

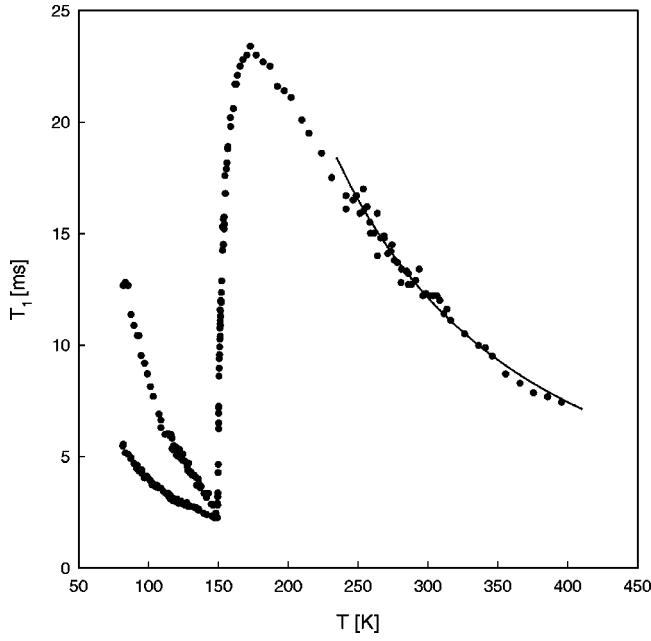


FIG. 2. Temperature dependence of T_1 in the normal and IC phase. Solid line represents the fit to the data using $T_1 = AT^{-\lambda}$ with $\lambda = 1.8$ at high temperatures.

quency dependence of T_1 at two different temperatures.

V. DISCUSSION

From direct observation of Fig. 1, it is seen that the spectra intensity at the lower frequency is greater than that at the highest edge frequency. On the other hand from Fig. 2 it is observed that T_1 is higher for the less-intensity peak of the spectra and vice versa, in good agreement with the results of Sec. III C.

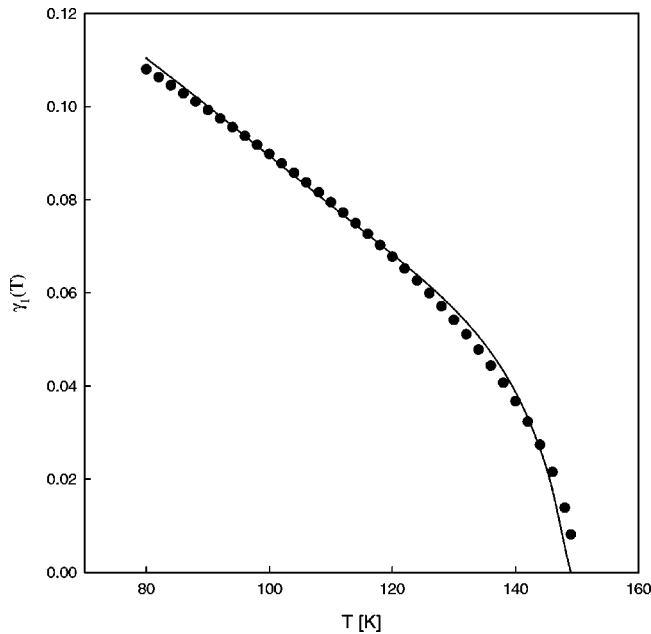


FIG. 3. Temperature dependence of the parameter γ_1 . Solid line: fit to the data using $\gamma_1 = c(T_I - T)^\beta$ with $\beta = 0.54$.

TABLE I. Relative intensity of the second-harmonic amplitude with respect to the first one calculated from the spectral-density profile and T_1 data.

T (K)	γ_1 (intensity)	γ_1 (T_1)
87	0.1	0.1
106	0.1	0.08
140	0.04	0.04
146.2	0.019	0.018

Recent results of the inelastic neutron-scattering study⁶ of the lattice-vibration spectra in the normal and incommensurate phases of BCPS have found an unusually low soft-mode damping. This important experimental evidence suggests that the spin-lattice relaxation process is dominated by Raman processes and not by direct processes as was stated previously.⁹

In this way a spline of both $T_1(T)$ data enables us to obtain, using Eq. (23), γ_1 as a function of temperature (Fig. 3). It is known from Eq. (4) that its behavior as a function of temperature in the mean-field theory should be

$$\gamma_1 = c(T_I - T)^\beta, \quad (24)$$

where T_I is the incommensurate transition temperature and $\beta = 0.5$.

A least-squared fit of data in Fig. 3 using this expression states

$$\begin{aligned} c &= 0.011 \pm 0.001, \\ T_I &= 149.6 \pm 0.1, \end{aligned} \quad (25)$$

$$\beta = 0.545 \pm 0.007$$

in good agreement with Landau's theory. In Table I is also shown a comparison at four different temperatures of the values of γ_1 calculated using the intensity of the spectra [Eq. (19)] and those using experimental T_1 data [Eq. (23)].

Knowing $\gamma_1(T)$, it is then possible to fit each $T_1(T)$ data adding only two free parameters

$$\frac{1}{T_1(-/+)} = pT^\lambda \left(1 - 2 \frac{\omega_{A0}}{\omega_{A\Lambda}} \right) [1 \mp 4 \gamma_1(T)], \quad \lambda \sim 2, \quad (26)$$

where it has been used that

$$J_{AA} = \kappa^{-5/2} \Lambda \left(1 - 2 \frac{\omega_{A0}}{\omega_{A\Lambda}} \right). \quad (27)$$

From Ollivier *et al.*⁶ $\omega_{A0} = \sqrt{2a(T_I - T) + \delta^2}$, $a = 350 \text{ GHz}^2/\text{K}$, $\delta = 80 \text{ GHz}$, and from Schneider *et al.*¹⁰ $\omega_{A\Lambda} \sim 4700 \text{ GHz}$.

A least-squared fit of data is shown in Fig. 4. In both cases the parameters are

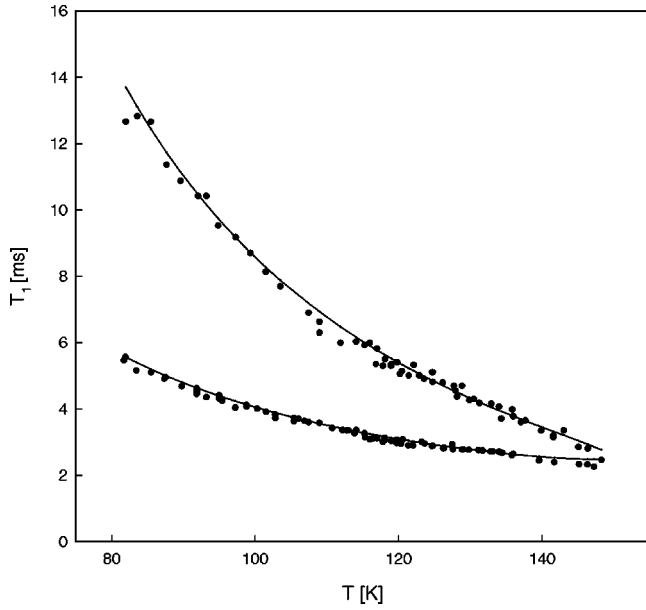


FIG. 4. Plot of $T_1(T)$ in the IC phase. Solid lines: data fit using Eq. (26).

$T_1(\nu_{high})$	$T_1(\nu_{low})$
$p = (6.6 \pm 0.8) \times 10^{-5}$	$p = (6.0 \pm 0.8) \times 10^{-5}$
$\lambda = 1.74 \pm 0.02$	$\lambda = 1.76 \pm 0.02$

As it is observed, both T_1 can be fitted with the same p and λ parameters. What makes the difference in the temperature behavior is the sign change in Eq. (26). Besides, the value of λ is in good agreement with $\lambda = 1.8$ obtained at high temperatures (Fig. 2).

Finally it is well known that the spin-lattice relaxation time varies over the incommensurate NQR line. From Eq. (13) it is possible to write down

$$W_I^\mu(X) = PX^3[X + 4\gamma_1(2X^2 - 1)] + Q[(X^2 - 1)^2(1 + 8\gamma_1X)] + Z[X(1 - X^2)(8\gamma_1X^2 + X - 2\gamma_1)], \quad (28)$$

where $Z \propto J_{A\varphi} + J_{\varphi A}$ and $Q \propto J_{\varphi\varphi}$ are unknown and P is evaluated using the above fitting parameters for the amplitude contribution at the corresponding temperature. On the other hand Eq. (16) allows to relate X with ν through

$$X = \frac{1}{2\gamma_1} - \sqrt{\frac{1}{4\gamma_1^2} + 1 - \frac{1}{\nu_1 A \gamma_1}(\nu_o + B\nu_1 - \nu)}. \quad (29)$$

Figure 5 shows the best fit to $T_1(\nu)$ data at $T = 118$ K and $T = 142$ K using these last two equations. The fit results show that the term that contains Z is very small and it can be neglected. The data are qualitatively well described and the fitting parameters are reported in Table II. It is worth noting that the frequency behavior is better described at high temperatures since at lower temperatures more harmonics term should be included in the IC modulation.³

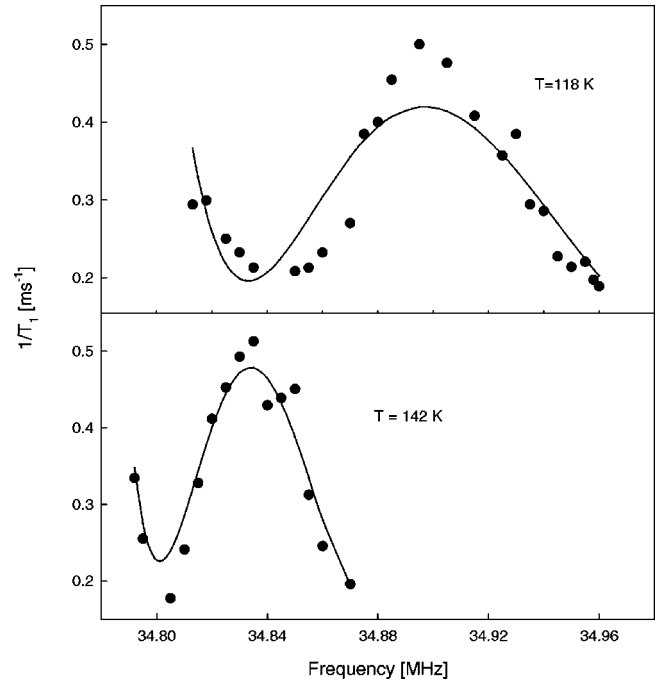


FIG. 5. Frequency dependence of T_1 at $T = 118$ K and $T = 142$ K. The solid line is a fit to the data using Eqs. (28) and (29).

VI. CONCLUSION

In the present work the calculations of NQR relaxation times, developed by Blinc, have been extended to include the effects of nonsinusoidal IC modulations. This model relates the equilibrium-displacement profile $\langle u(x) \rangle$ and the spatial-fluctuation profile $\delta u(x)$ with two NQR observables: the spectral density $f(\nu)$ and the spin-lattice relaxation time T_1 , respectively. These relations provide two independent and equivalent ways to obtain the relative intensity of the second harmonic with respect to the first one [i.e., $\gamma_1(T)$, see Eq (4)] of the IC distortion. It has been also shown that, when nonsinusoidal IC modulations are present, the NQR spectra is not symmetric and the peak of the spectra that has lower intensity always has a larger T_1 and vice versa.

The theoretical calculations are in good agreement with BCPS NQR data. They enable to explain not only the asymmetric in the edge-peak intensities of the NQR spectra, but also the temperature dependence of T_1 as well as its frequency dependence, when Raman processes are considered to dominate relaxation as is indicated by neutron-scattering evidence. It is important to remark that just a sign change in Eq. (26) for Raman processes allows to describe $T_1(T)$ at both edges of the spectrum. On the other hand an excellent agreement was found between γ_1 obtained from the analysis of the spectral profile at different temperatures and that ob-

TABLE II. Fitting parameters of the frequency dependence of the transition probability at 118 K and 142 K.

T (K)	Q (ms^{-1})	$A\nu_1$ (Mhz)	$\nu_o + B\nu_1$ (Mhz)
118	0.42	0.102	34.910
142	0.46	0.052	34.839

tained from $T_1(T)$ data. Moreover the experimental curve obtained for $\gamma_1(T)$ from the $T_1(T)$ data shows that its temperature dependence agrees with that expected from the simplest Landau theory of the incommensurate phase.

ACKNOWLEDGMENTS

The authors wish to express their thanks to CONICOR of Córdoba and SeCyT-UNC for financial support.

¹R. Blinc, Phys. Rep. **79**, 331 (1981).

²Herman Cummins, Phys. Rep. **185**, 211 (1990).

³J. Schneider, C. Schurrer, A. Wolfenson, and A. Brunetti, Phys. Rev. B **57**, 3543 (1998).

⁴J. Schneider, A. Wolfenson, and A. Brunetti, J. Phys.: Condens. Matter **6**, 11 035 (1994).

⁵F. Zuñiga, J. Perez-Mato, and T. Breczewski, Acta Crystallogr., Sect. B: Struct. Sci. **B49**, 1060 (1993).

⁶J. Ollivier, J. Etrillard, B. Toudic, C. Ecolivet, P. Bourges, and A. Levanyuk, Phys. Rev. Lett. **81**, 3667 (1998).

⁷A.D. Bruce and R.A. Cowley, J. Phys. C **11**, 3609 (1978), We follow closely the notation developed in this reference.

⁸F. Borsa and A. Rigamonti, in *Magnetic Resonance of Phase Transition*, edited by C. Poole, Jr. and H. Farach (Academic, New York, 1979).

⁹R. Blinc, T. Apih, J. Dolinsek, and U. Mikac, Phys. Rev. B **51**, 1354 (1995).

¹⁰J. Schneider, H. Panepucci, M. dos Santos, C. Meriles, and A. Nunes, J. Phys. Soc. Jpn. **68**, 37 (1999).